Habitat Use of the Northern Bottlenose Whale (*Hyperoodon ampullatus*) near Jan Mayen, North Atlantic

K. Y. Woo [1,2], S. Isojunno [1,3], P. J. O. Miller[1,*]

[1]Sea Mammal Research Unit, Scottish Oceans Institute, University of St. Andrews, St. Andrews, Fife KY16 8LB, UK

[2]Present Address: Rm8, 17/F, 31-39A Waterloo Road, Kowloon, Hong Kong

[3]Present Address: Centre for Research into Ecological and Environmental Modelling (CREEM), University of St Andrews, The Observatory, Buchanan Gardens, St. Andrews, KY16 9LZ

*Corresponding author. Tel: +44 (0)1334 463554; E-mail address: pm29@st-andrews.ac.uk

1. Abstract

Habitat use of the northern bottlenose whale (*Hyperoodon ampullatus*) in the Northeast Atlantic remains poorly understood. This study aimed to identify locally utilised habitat features and to create predictions of northern bottlenose whale habitat use over a wider area around the island of Jan Mayen, Norway. Bottlenose whales were sighted regularly near Jan Mayen in June 2014-2016, at higher rates than over a wider study region reported in other studies, indicating the Jan Mayen habitat may be a hotspot of bottlenose whale presence in early boreal summer. Habitat models were created by fitting Generalized Additive Models (GAMs) of selected environmental variables to sighting occurrence and additional whale sightings given first encounter (total number of sightings - 1) recorded in June 2014-2016. Higher occurrence was estimated at steeper topography and April-average chlorophyll concentration below 0.4 mg m^{-3}. Additional whale sightings given first encounter were predicted to be higher at water depths (<1,000m) with steep topography, and deeper water depths between 1,300m and 2,000m with gentle seafloor slope. Spatial predictions largely corresponded with field observations which indicated high usage around the submarine canyon regions in the east and southeast of Jan Mayen Island. This study highlighted the likely importance of steep and deep bathymetric features in shaping patterns of habitat use of this deep-diving species. Predictions of habitat use over a wider area not covered by the analyzed surveys require validation, but could inform conservation and management efforts to minimize spatial overlap between potential high-use areas and potentially-disruptive anthropogenic activities.

Key words: Habitat use; Habitat models; Beaked whale; Multi-model inference; Generalized additive models; Bathymetry; Opportunistic sampling; North Atlantic

2. Introduction

Patterns of habitat use reflect the way animals utilize the geographic and biological distribution of resources (Krausman 1999). For wide-ranging mobile animals such as cetaceans, responses to environmental variability are readily reflected by spatial and temporal changes in distribution and habitat use patterns (Forney 2000). Species-habitat modelling can serve as a powerful and flexible tool to explain and predict such varying patterns of habitat use under ecologically dynamic processes (Forney 2000, Redfern et al. 2006), and thus allow inference of high-use areas with respect to associated environmental features (Guisan & Zimmermann 2000). Together with knowledge of distribution and abundance (Hooker et al. 1999, Cañadas et al. 2005, Redfern et al. 2006, Rogan et al. 2017), understanding habitat use sets a foundation for effective conservation and management. For example, habitat-based mitigation measures can reduce spatial and temporal overlap between areas of high animal occurrence and anthropogenic activities (Rogan et al. 2017). However, it can be challenging to obtain required field data for offshore deep-diving marine mammals such as beaked whales because of financial and logistical constraints involved studying these elusive species (Forney 2000).

Cetacean distribution within their feeding areas is expected to be primarily correlated with the abundance and distribution of their prey (Kenny et al. 1996, Hátún et al. 2009), which may be largely unknown (e.g., Isojunno et al., 2012). Therefore, environmental variables are usually included in habitat models as proxy measurements of prey availability (Redfern et al. 2006, Rogan et al. 2017). The northern bottlenose whale *Hyperoodon ampullatus* (Family: Ziphiidae, beaked whales) (Forster 1770) (referred as "bottlenose whales" hereafter) is a deep-diving cetacean for which scarce information on distribution and habitat use is available, owing to biological factors such as pelagic habitat (Hooker et al. 2002, Ramírez-Martínez et al. 2020) and long and deep dives (Hooker & Baird 1999). Previous studies indicate they feed primarily on the benthic living cephalopod *Gonatus fabricii*, the most abundant deep-water squid in Arctic and sub-Arctic (Bjørke 1995), and occasionally on other squid species and fish (Kastelein & Gerrit, 1991, Lick & Piatkowski 1998, Hooker et al. 2001, Fernández et al 2014). Knowledge of population trends and

distribution of this species is principally based upon historical whaling records (Whitehead et al. 2021) and recent research on the uniquely well-studied population in the Gully, Nova Scotia, Canada (Hooker 1999, Gowans et al. 2000). Likely driven by prey distribution and availability, bottlenose whales tend to favor open waters ≥ 1,000m along the continental slope (Benjaminsen 1972, Whitehead & Hooker 2012), the primary habitat of large and mature *G. fabricii* (Bjørke 2001).

More than 65,000 bottlenose whales were taken during commercial whaling since the 1850s (Reeves et al. 1993), and this has severely depleted the global population, likely causing it to remain well below historical levels (Whitehead et al. 2021) given their slow reproductive rate (Feyrer et al. 2020). In combination with high susceptibility to pervasive anthropogenic threats, including disturbance from underwater noise (Miller et al. 2015, Wensveen et al. 2019) and risk of bycatch, bottlenose whales have been classified as 'Near Threatened' by the IUCN Red List (Whitehead et al. 2021). As yet there is no regional or national conservation framework established for this species or its habitat outside the Gully Marine Protected Area (Whitehead & Hooker 2012), where bottlenose whales of the Scotian Shelf are found to be genetically distinct from other North Atlantic populations (COSEWIC 2011, Feyrer 2021, de Greef et al. 2022, Einfeldt et al. 2022).

In the Northeast Atlantic where bottlenose whales were most hunted (Whitehead & Hooker 2012), estimates from the 1990s indicated roughly 40,000 individuals (NAMMCO 1995), with high-latitude (over 60 °N) population potentially forming four distinct stocks off: i) northern eastern Greenland, Iceland, Jan Mayen and Faeroe Islands, ii) Andenes, Norway, iii) Møre, Norway, and iv) Svalbard (Benjaminsen 1972, Whitehead & Hooker 2012). Recent sighting data have documented bottlenose whales in waters south-east of Svalbard, and along the Knipovich Ridge (Storrie et al. 2018). High density areas were identified in shipboard line-transect surveys between the British Isles and Greenland, but few or no sightings were made in historic whaling grounds off Svalbard, Andenes and Møre, despite effort in those areas (Ramírez-Martínez & Hammond 2019). The northern limits for this species in the eastern North Atlantic may be in a state of flux due to changing ice conditions (Whitehead et al. 2021).

A broad description of habitat use in the northeast Atlantic based upon shipboard surveys conducted in 1998-2015 found a positive effect of depths from 800 to 2,000m on bottlenose whale density, with waters shallower than 500m having a negative effect on whale density (Ramírez-Martínez & Hammond 2019). Other significant factors included seafloor aspect, sea surface temperature and mixed layer depth in June, salinity in August, sea surface height in July, and chlorophyll *a* in April.

From 2014 to 2016, the 3S^3-ORBS (Sea Mammals and Sonar Safety – Off -Range Beaked whale Study) project (Miller et al. 2014, 2015, 2016) conducted sailboat-based surveys in the waters off the Island of Jan Mayen to collect visual and animal-attached tag data of bottlenose whales. During the survey period in June of each year, animals were routinely sighted along the Jan Mayen submarine canyon, mainly to the north and southeast of the Island of Jan Mayen. The surveyed area is topographically dominated by the West Jan Mayen Fracture Zone which forms a steep submarine canyon (1,200 – 3,800m, Fig.1) (IHO-IOC 2017), resulting in steep and deep bathymetric profile close to the north coast of Jan Mayen Island. Oceanographically, the region is characterised by the Nordic Sea circulation, which consists mainly of the warm and saline Norwegian Atlantic current and, cold and fresh East Greenland current flowing in opposite directions (Piechura & Walczowski 1995, Schepper et al. 2015). The interface between these currents forms the Arctic Jan Mayen front (Piechura & Walczowski 1995**,** Erga et al. 2012, IMBER IPO 2012**,** Børsheim et al. 2014), which creates a strong thermohalocline gradient within water column from 0 to 200m (Piechura & Walczowski 1995). The spring bloom off northern Jan Mayen is found to last longer and reach higher chlorophyll concentration compared with other regions on the Arctic side of the front (Børsheim et al. 2014).

The aims of this study were: 1) to use bottlenose whale sightings data to quantify habitat use near Jan Mayen and identify key static and dynamic environmental correlates of bottlenose whale presence within a habitat-use model; and 2) to apply the habitat-use model to predict potential bottlenose whale habitat use pattern across a wider area of the Greenland Sea.

3. Materials & Methods

3.1 Surveyed Area and Wider Prediction Area

The surveyed area encompassed a marine region covered by major survey effort tracks around the Island of Jan Mayen in the Norwegian Sea (Fig. 1), delimited by latitudes 70°N and 71.5°N, and by longitudes 5°W and 9.5°W. Model predictions were made over a wider rectangular marine region demarcated by latitudes 68°N and 72°N, and by longitudes 1°W and 17°W, based on sightings made within the surveyed area.

3.2 Visual Sighting Data Collection

Visual sighting data of bottlenose whales were collected in June in 2014, 2015 and 2016 (Table 1), with search effort concentrating along the submarine canyon going from north to southeast of the Jan Mayen Island (Fig. 1). The visual surveys were conducted by two dedicated observers from the deck whenever weather conditions permitted. Both observers scanned with naked eyes from bow to stern with one searching across the starboard and the other across the port of the boat, together covering 360° around the vessel. Binoculars were used to confirm whale species and location once an animal was spotted.

When a sighting was made, the time, whale location (latitude and longitude), estimated sighting distance, bearing, group size, animal heading, level and duration of seeking (behavioural indication of attractive movement towards the research vessel, as suggested by Whitehead & Hooker (2012)) were recorded. Vessel GPS location and speed were automatically logged every five sec in 2014 and 2015, and every sec in 2016.

Boat speed was maintained between 4 and 7 knots during survey, which was approximately double of the normal swim speed of bottlenose whales (~ 5 km/h, Kastelein & Gerrits 1991). It could therefore be assumed that animals were stationary when visual sampling took place, and any positive bias due to repeated counting of the same individual or group was minimized (Glennie et al. 2015).

Following a sighting, the whales were often approached for tagging. If successful, the tagged whale would be tracked for the duration of the tag deployment. Sighting and effort data during tagging and tracking periods were excluded from the analyses.

3.3 Calculation of Survey Effort

Survey effort, which is a measure of locations searched, was first quantified to account for the spatial and temporal heterogeneity of the sampling, which was opportunistic in the sense that it was determined mostly by weather and logistics for tagging, rather than a-priori distribution survey design. Only effort data with Beaufort sea state lower than 5 and visibility greater than 2 km, when observers actively looked for whales during on-effort status, were considered for further analysis. These criteria were used to reduce perception bias caused by poor weather conditions. The selected tracks were then divided into segments of 12.5 km with each segment representing a spatial unit of observer effort. The 12.5 km segment length was determined considering the size of study area and the average spatial resolution of explanatory variables, so that covariate values were not over-averaged within each effort segment.

3.4 Tabulation of Static and Dynamic Environmental Variables

Effort segments were populated with covariate set of grid pixels on which the centroid point of each segment landed, based on the assumption that whale sighting and its corresponding effort segment shared the same set of environmental variables. A grid layer of 1470 pixels (12.5 x 12.5 km) was overlaid on the wider prediction area to standardize the spatial resolution of environmental variables for each grid cell. As grid size was the same as length of effort segment, candidate covariates were not over-averaged within effort segment, and were also not averaged over several effort segments. Environmental predictors to be evaluated for inclusion in habitat use models consisted of five static, four dynamic, and two temporal covariate variables (Table 2).

3.4.1 Static Environmental Variables

120 Bathymetry was summarised as water depth (IOC IHO and BODC 2003), seafloor slope, aspect and
121 distance from 2,000 m depth contours. It was expected that underwater topography would play a
122 considerable role in explaining the observed pattern of whale habitat use off Jan Mayen, since water depth
123 is a good predictor of *H.ampullatus* distribution in the northeast North Atlantic (Ramírez-Martínez &
124 Hammond 2019) and above the Gully off Nova Scotia (Hooker 1999, Hooker et al. 2002), as well as
125 beaked whale distribution and abundance in the North-East Atlantic (Rogan et al. 2017). Mean depth –
126 slope interaction term was also included as predictor variable, as the interaction between depth, slope and
127 bottlenose whale sightings in the Gully was found to be significant (Hooker 1999, Hooker et al 2002).
128 Predicted core area for bottlenose whales in north-western Atlantic was found to be characterized by
129 aspect (Compton 2004). Distance from 2,000 m depth contour is significantly associated with beaked
130 whale distribution in northern east Atlantic (Rogan et al. 2017).

131 Distribution of *G. fabricii* is found to be strongly related to the Norwegian current system. The
132 Norwegian Atlantic current brings *G. fabricii* juveniles northward to waters between Jan Mayen and
133 Vesterålen (Wiborg et al. 1982), while deep-sea adults might join the East Greenland current to reach Jan
134 Mayen (Bjørke 1995). The proximity to the frontal boundary, which appears to be geographically steady
135 across the study period (Raj et al. 2019, Skagseth et al. 2022), is a good predictor of habitat use of beaked
136 whales and squid-feeding sperm whales (*Physeter macrocephalus*) off the North-East US (Waring et al. 2001).

137 *3.4.2 Dynamic Environmental Variables*

138 Dynamic variables including chlorophyll *a* concentration (Chla), sea surface temperature (SST), sea
139 surface height (SSH), and salinity (SA) were included as proxies of cephalopod distribution given the squid
140 species, including *Gonatus,* feed on amphipods and copepods (Bjørke 1995). Since Chla, SST and SSH are
141 more likely to reflect plankton growth rather than squid or whale distribution directly (Eppley 1972),
142 two-month lagged values (April-averaged) were used to account for the energy transfer across trophic
143 levels. For SA, June-averaged values without time lag were used as distribution of *Gonatus* squid is found
144 to be strongly associated with high SA level (above 35 ppt) in Atlantic waters (Bjørke 1995).

145 Solar elevation and survey year were also examined to capture any temporal pattern of whale habitat
146 use: the former reflected the effect of hourly change in sun position relative to the horizon, while the
147 latter reflected annual variation between survey years. Elevation angle was calculated based on the
148 algorithm presented by Michalsky (1988) and verified using NOAA Solar Calculator (Global Radiation
149 Group 2017).

150 ***3.5 Bottlenose Whale Habitat Modelling***

151 *3.5.1 Detection Function Analysis*

152 Distance sampling analysis was performed to estimate the detection function for bottlenose whales,
153 using Distance package ver. 0.9.6 (Marshall et al. 2016) in statistical software R ver. 3.4.1 (R Core Team
154 2017). This technique is commonly adopted for distribution and abundance estimates in cetacean studies
155 (Hammond et al. 2002, Hammond et al. 2009, Embling et al. 2010, Hammond et al. 2013, Rogan et al.
156 2017). Sightings that involved attraction to the research vessel were excluded from this analysis.
157 Perpendicular distance was re-calculated, followed by truncation of sighting data at a distance to improve
158 model goodness-of-fit while retaining as many data as possible (Buckland et al. 2001). Model fit was
159 examined and compared using QQ plots and goodness-of-fit tests (Buckland et al. 2004).

160 Conventional distance sampling (CDS) models (Buckland et al. 2001) with half-normal and hazard-rate
161 key functions were fit and compared based on Akaike Information Criterion (AIC, Akaike 1992) and QQ
162 plots. The model fits detection probability as a function of perpendicular distance from transect lines.
163 Multi-covariate distance sampling (MCDS) (Marques & Buckland 2003) models were then run to
164 incorporate the potential effects of environmental and sighting conditions in addition to detection distance.
165 Group size and Beaufort sea state were examined to account for covariate-related heterogeneity in
166 detection probability by post-survey stratification of data (Marques & Buckland 2003). Since there were
167 not many sightings with group size larger than four, and the environmental conditions at multiple Beaufort
168 scales were similar, some sightings were grouped together for MCDS modelling. CDS and MCDS models

with the best functional form (either half-normal or hazard-rate) were examined and compared using AIC and Cramer-von Mises test (that is, goodness-of-fit test to compare the exact and asymptotic distribution, Cramér 1928), and the best-fitting model was adopted for the estimation of detection probability and associated effective strip width (ESW). Significant effects of group size and/or sea state (if any) would be taken into account in habitat models via the offset, which was calculated as the effort segment length multiplied by twice the effective strip width.

3.5.2 Sighting Occurrence and Additional Sightings Response Variables

Wildlife count data often contain larger number of zeros (absences of detection) than expected by classical count probability distributions, such as the Poisson distribution. Zero-inflation can be caused by multiple factors, including experimental design, sampling variability, and the size and behaviour of animal population of interest (Blasco-Moreno et al 2019). In this study, zero-inflation may have been partly driven by the long dive duration of the study species, which reduces their availability to visual detection at water surface. Here, the sightings data appeared to be zero-inflated according to Vuong test results (Vuong 1989). A two-model approach was therefore adopted to accommodate for the zero-inflated nature of sightings data: i) sighting presence/absence per segment was first modeled with binomial model for the prediction of occurrence, i.e., expected probability of whale sighting presence/absence, followed by ii) the number of additional whale sightings given first encounter i.e., zero-truncated counts of sighting conditional on presence, per segment fitted to a Poisson model. The two-step model approach (probability function detailed by Zuur et al. (2009) as their Equation 11.24), also known as hurdle model developed by Cragg (1971), has been commonly applied in ecological studies aiming to predict relationships between animal sighting data and environmental variables (Agarwal 2002, Barry & Welsh 2002, Potts & Elith 2006, Mellin et al. 2012, Smith et al. 2019). It has also been found to outperform other regression models in terms of model fit between observations and model predictions (Potts & Elith 2006), with flexibility allowing for potential different drivers of animal occurrences and counts.

As linear cetacean-habitat relationships are uncommon, sighting presence/absence and additional sightings were fitted with generalized additive models (GAMs, Hastie & Tibshirani 2006) within the mgcv (ver 1.8-28, Wood 2016) library in R (ver. 3.4.1).

3.5.3 Modelling Occurrence of Whale Sightings

In a first step to understand the effect of each covariate, univariate GAMs were fit within the mgcv library in R (ver. 3.4.1) to relate sighting presence/absence per segment to each predictor variable. Sighting presence/absence per segment was assumed to follow a Bernoulli distribution as an animal was either present or absent in a particular effort segment. The expected probability of whale sighting occurrence in the i^{th} segment, $E[y_i]$, is formulated as (Hedley et al. 1999):

$$E[y_i] = g^{-1}[\beta_0 + \sum f(z_i)] \quad (1)$$

Where $g()$ is the link function, β_0 is the intercept to be estimated, f represents the smooth functions of explanatory covariates, and z_i denotes the value of the explanatory variable in the i^{th} effort segment. Probit link function was chosen for the global binomial model as it had smaller scores of unbiased risk estimator (UBRE) in most univariate GAMs. Working in a similar fashion as AIC, a smaller UBRE score indicates better model fit (Shadish et al. 2014). Most covariates were included as smooth terms, except for 'year' which was treated as a factor, and the interaction term of mean depth and slope which was specified as a tensor product interaction allowing covariates to be included at different scales (Wood 2006).

The maximum number of knots (i.e., degrees of freedom, joining successive spline of smooth along the x-axis) was manually set as eight as the sample size was much larger than 100 (Thomas 2015), and the optimal degree of smoothing was chosen by cross-validation. In addition, covariate terms were specified as thin plate regression splines, whose shrinkage component penalizes smooth parameters to zero if no signal is found (Wood 2016). These allow the degrees of freedom to be included as part of the model selection process (Rogan et al. 2017).

Correlation among non-normally distributed covariates was examined by Spearman's rank collinearity test in R (R Core Team, 2017)(ver. 3.4.1). For highly correlated variables ($r>0.5$ or $r<-0.5$), only the one which explained more of the deviance, with a lower UBRE score and was more informative and ecologically influential (i.e., with more direct ecological impacts) was retained based on the univariate model results. This selection process improves model reliability by ensuring that the assumption of independence among explanatory variables is not violated (Thomas 2015). Selected covariates from the univariate models were included in a global, multivariable, model for the occurrence model selection.

3.5.4 Binomial Model Selection and Model Averaged Predictions

Since GAMs with different degree of smoothness are not nested, global model selection instead of stepwise selection was performed within the MuMIn (Barton 2015) library in R. The smooth terms of latitude and longitude was excluded as candidate covariates prior to model selection, given the spatial coverage of the surveyed area was uneven in terms of coordinates, and model estimates for wider prediction area would thus be highly uncertain. Models with all other possible covariate combinations were compared by AICc (that is, adjusted AIC with correction for sample size, Cavanaugh 1997) and model weight. Model fit was also examined by UBRE score, adjusted R-squared value (reflects the proportion of variance explained) and the percentage of deviance explained by model.

Standard model diagnostics tests (residual plots, influence and leverage plots) were then performed for the best binomial GAM, although the binary nature of response variable makes residual plots (except for QQ plots) difficult to interpret. Serial residual correlation was checked using Durbin-Watson test (Durbin & Watson 1971) and illustrated by autocorrelation function (ACF) plot (Fox et al. 2016) after model selection as it could not be incorporated into GAM together with the shrinkage smooth terms. A particular time–lag with p-value<0.05 in Durbin-Watson test or with ACF score exceeding the threshold values for statistical significance (illustrated as horizontal dotted lines in ACF plot) was considered to imply serial correlation (Thomas 2015).

Uncertainty in model selection due to the large number of covariate combinations was addressed by model averaging (Burnham & Anderson 2002), in which spatial prediction was made based on a confidence set of models with ΔAICc less than two. Model-averaged predictions of sighting occurrence and associated coefficients of variation were calculated for each prediction grid. The relative importance of each predictor variable was calculated by the summation of Akaike weights. Model-averaged predictions of sighting occurrence were then plotted throughout the range of each significant covariate (with $\alpha = 0.05$), given other predictor variables were fixed at their mean values.

3.5.5 Modelling the Number of Additional Whale Sightings Given First Encounter

Similar to the GAM for sighting occurrence, the respective relationships between number of additional sightings per segment (provided there was at least one sighting) and each predictor variable were first modeled as univariate GAMs. This approach is designed to independently model additional number of whale sightings given first encounter as a response parameter, which is not accounted for in the occurrence-only model. The response variable was assumed to follow a Poisson distribution which required the estimation of a single rate parameter λ. The expected number of additional whale sightings in the i^{th} segment, $E[x_i]$, can also be calculated by formula (1), except that the log link function was specified due to its lower UBRE score. An interaction term between mean depth and slope was also included. The maximum degrees of freedom were set manually, and over-fitting prevented in the same way as for the occurrence model. Model selection and diagnostics were carried out following the same criteria and procedures as for the occurrence model, with the same covariate set as suggested by univariate models and covariate collinearity test being specified in the global Poisson GAM. Model-averaged predictions of the number of additional whale sightings given first encounter, coefficient of variation and covariate effects were estimated and visualized the same way as the occurrence predictions. It should be noted that group size of whale sighting was not included in the Poisson GAM, as it is potentially correlated with social factors other than environmental variables, e.g., male bottlenose whales appeared to form

stronger associations with con-specifics in their own age classes compared with females and immature individuals (Gowans et al. 2001).

3.5.6 Zero-inflated Poisson Location-scale Model

The two-model estimates of habitat use relationships were validated by zero-inflated Poisson location-scale model within the mgcv library in R (ver. 3.4.1). The zero-inflated GAM consists of two linear predictors: one controls the probability of occurrence with logit link function, while the other controls the Poisson parameter given first encounter with log link function (Wood 2016). The first and second formulae of the model specify the multivariate response and the linear predictor structure respectively for Poisson and binomial parameters (Wood 2016). Here, the response variable was simply the number of whale sightings made per segment. Covariate sets for the best models of additional sightings given first encounter, and sighting occurrence were specified in the first and second formulae respectively. Given comparable model assumptions such as $\alpha = 0.05$, model estimates of the zero-inflated GAM were expected to be similar to those of the two-model hurdle approach.

3.5.7 Spatial Prediction of Habitat Use

The predicted pattern of habitat use in relation to the environmental covariates for a wider area (Fig. 1) was obtained by quantifying environmental covariates retained in our near Jan Mayen habitat model. Model-averaged estimates of sighting occurrence and number of additional whale sightings plus one were multiplied (i.e. occurrence probability x sightings, so as to calculate the predicted total number of whale sighting for each grid with the observed number of sightings) for each prediction grid. Standard error (SE) was first calculated as the square root of sum of estimated variances of occurrence and additional sightings given first encounter (Buckland et al. 2001), and it was then converted to coefficient of variation as a measure of prediction uncertainty.

4. Results

A total of about 4,000 km of survey distance was included in the analysis, with a roughly equal distribution of effort across the three years 2014-2016. Northern bottlenose whales were regularly sighted in the surveyed area each year with a mean survey distance per sighting of approximately 18 km (Table 1). The average group size of sightings was 3.1±1.4, resulting in a mean survey distance per individual of 5.8 km off Jan Mayen Island, compared to 1,463.9km in Norway and 104.6 km in Iceland-Faroes as per Ramírez-Martínez and Hammond (2019).

4.1 Detection Function Analysis

Twenty-six of 220 sightings were scored in the field as attracted to the research vessel (labelled as 'strong seekers' as part of the field data collection) and discarded prior to detection function modelling. The truncation distance was set to 700 m, retaining approximately 167 sightings, which was ~85% of non-seeking sightings. The final best model for detection probability was a hazard-rate CDS model as a function of perpendicular distance (Fig. 2), followed by MCDS models all with ΔAIC>2 (Table 3). The average detection probability of bottlenose whales given the 700 m truncation distance was estimated to be 0.33 (CV = 0.15), for an effective half-strip width of 231 m or effective strip width of 462 m. The 0.33 correction factor was applied to all effort segments assuming that the survey years and whole surveyed area was homogenous in terms of detection probability. No offset or effective strip width information was fitted to habitat models for occurrence and additional sighting estimates.

4.2 Habitat Modelling

Based on the results of the covariate collinearity test and univariate modelling of both response variables (sighting presence/absence and additional sightings), global models with seven covariates (including mean depth, distance from Arctic front, April chlorophyll concentration, April sea surface temperature, slope, solar elevation and aspect) and the tensor product term of depth-slope interaction were established for model selection.

4.2.1 Occurrence of Whale Sightings

The best occurrence model (with the lowest UBRE score and AIC) retained bathymetric slope, April chlorophyll concentration, April sea surface temperature, and a topographic interaction of depth with slope, explaining 8.4% of the deviance (Table 4). With the first two variables gaining statistical support ($p<0.05$) also in the zero-inflated Poisson location-scale model, sighting occurrence was found to increase with steeper topography (Fig. 3a). Whale sighting occurrence was predicted to correlate with lower April concentration of chlorophyll (below 0.4 mg m^{-3}), with greater prediction uncertainty above 1 mg m^{-3} (Fig. 3b). Sea surface temperature (SST) became insignificant ($p>0.05$) when the same covariate set was specified in the zero-inflated Poisson GAM, indicating that the effect of SST was not robust. The model was interpreted without incorporating any autoregressive structure (AR(1) or ARIMA) given general additive mixed models (GAMMs, Chen 2000) are reported to perform poorly with binary data (Wood 2016). Nevertheless, it should be noted that standard error (SE), confidence interval (CI) and coefficient of variation (CV) quantifying the uncertainty in covariate effects were likely to have been somewhat underestimated without incorporating any autoregressive structure. Occurrence model diagnostics are detailed in *Supplementary Materials.*

4.2.2 Average Estimates of Occurrence Based on the Confidence Set of Models

The confidence set consisted of 49 models with ΔAICc<2, which accounted for 70.4% of total Akaike weights. Sea surface temperature in April and chlorophyll concentration in April were respectively the most and second most important variables with high relative importance (with summed Akaike weight of 1 and 0.95, respectively) and were included in nearly all models among the confidence set. Maximum slope was moderately important (with relative importance of 0.67) and was retained in about 60% of all models among the confidence set.

Model-averaged predictions of occurrence plotted against each statistically supported covariate, with other explanatory variables fixed at their mean values in the data, are given in Fig. 3. Similar to the best occurrence model estimates, higher occurrence was predicted at steeper topography (Fig. 3c) and April chlorophyll concentration below 0.4 mg m^{-3} and above 1 mg m^{-3}, with greater prediction uncertainty

above 1 mg m^{-3} (Fig. 3d). Spatial estimates of sighting occurrence were based on model-averaged predictions, and are further detailed in *Supplementary Materials*.

4.2.3 Number of Additional Whale Sightings Given First Encounter: GAM results

The number of additional whale sightings given first encounter (total number of whale sightings – 1) was modeled as a function of the same covariate set (see section 4.2) in the global Poisson GAM. The final best Poisson model with the lowest UBRE score and AIC retained all covariates except for solar elevation, while the six explanatory variables and one topographic interaction term together explained 23.4% of the deviance (Table 4). With depth-slope tensor product term being the only statistically supported variable at 5% level also in the zero-inflated Poisson GAM, the number of additional whale sightings given first encounter at different water depths appeared to depend on seafloor slope: steep topography increased the expected additional number of whale sightings given first encounter at shallower water depths (<750 m), while more additional whale sightings were estimated in deep waters (about 2,000 m) with gentle slopes (Fig. 4). Distance from the Arctic front lost statistical support ($p>0.05$) when the variable was specified in the zero-inflated Poisson GAM, indicating that the effect of this predictor was not robust. As GAMM could not effectively correct for serial correlation in this case, the best additional sightings model was also interpreted without any autoregressive structure. Standard errors, confidence intervals and coefficients of variation were also likely to have been underestimated under serial correlation. Model diagnostics for Poisson GAM are further explained in *Supplementary Materials*.

4.2.4 Average Estimates of Number of Additional Whale Sightings Given First Encounter - Confidence Set of Models

The confidence set included 25 models with ΔAICc<2, accounting for 61.7% of total Akaike weights. Depth-slope interaction term, distance from Artic front and depth were the three most important variables, and they were retained in almost all models among the confidence set with very high relative importance (Akaike weight ~1).

358 Model-averaged predictions of additional whale sightings given first encounter were plotted throughout
359 the range of each important covariate in Fig. 5. The effect plot for tensor interaction term between mean
360 depth and slope (Fig. 5a) illustrated that more bottlenose whales were estimated at water depth between
361 1,000 m and 2,500 m with flat topography, whereas those found at water depth shallower than 1,000 m
362 preferred steeper seafloor slope. The standard error (SE) values of model predictions made for shallow
363 water depths with steep slopes were high given the estimates were dominated by few data points (Fig. 5b).

364 *4.2.5 Wider Area Habitat Use Prediction*

365 The predicted pattern of potential habitat use based on estimates of sighting occurrence multiplied by
366 estimated number of total whale sightings (additional number of whale sightings given the first encounter
367 plus one) was concordant with whale sightings recorded in the surveyed area along the West Jan Mayen
368 Fracture Zone: higher sighting rates were predicted in the southeast of the submarine canyon and off the
369 Jan Mayen Island (Fig. 6). Higher numbers of whale sightings were predicted in areas off the northwest of
370 the Island of Jan Mayen, which were similar to the occurrence model estimates. Fewer sightings were
371 predicted in the southeast corner of the wider prediction area and coastal waters south of Jan Mayen,
372 which was consistent with the spatial estimates of whale sighting occurrence model. Higher prediction
373 uncertainty (that is, higher value of coefficient of variation) was estimated southeast corner of the wider
374 prediction area, matching the lower survey effort in the area.

5. Discussion

375 Regular bottlenose whale sightings were made yearly during the survey efforts in June 2014-2016,
376 indicating an overall high level of use of the surveyed area at those times. The average group size sighted
377 was about 3 individuals, which was consistent with the group sizes observed near Jan Mayen in June 2013
378 (Miller et al. 2015a) though some larger group sizes were noted by Ramírez-Martínez and Hammond
379 (2019, see their Figure 22). While the sighting platform of this study was likely less effective than the
380 shipboard double-platform of the study by Ramírez-Martínez and Hammond (2019), the effective strip

widths for both studies were similar (Ramírez-Martínez, per. comm. November 2021). The much shorter mean survey distance per animal in our study (6 km/whale, Table 1) versus that of the wider regions covered by Ramírez-Martínez and Hammond, 2019 (105 to 1,460 km/whale, see their Table 2) therefore indicates that Jan Mayen in the period surveyed had a relatively high sighting rate of northern bottlenose whales.

5.1 Species-habitat Modelling

5.1.1 Model Estimates and Significant Environmental Correlates

Binomial model results indicated that seafloor slope and April chlorophyll concentration were significant correlates of bottlenose whale sighting occurrence within the wider prediction area during June 2014 to 2016. Preference for steep bathymetry (Fig. 3c) around the Jan Mayen Island is consistent with bottlenose whale habitat preference off eastern Canada: higher whale encounter rate (which is, the number of encounters divided by number of hours of effort) was correlated with steeper seafloor slope within the Gully submarine canyon (Hooker et al. 2002). The estimated relationship may be driven by the ontogenetic descent in juvenile *Gonatus*, which performs vertical migration from shallow water to depths over 1,000 m upon maturity (Hooker 1999, Bjørke 2001). This could attract whales to deeper water in order to feed on prey with greater body size. The probability of whale sighting was also found to be higher in concentrations of chlorophyll below 0.4 mg m^{-3} in April (Fig. 3d), which was also predicted in the zero-inflated Poisson GAM. This pattern is different from the chlorophyll relationship typically observed in other cetacean species: animal distribution positively correlates with productive waters with higher sea surface chlorophyll concentration (Smith et al. 1986, Redfern et al. 2008), an indirect indication of high prey abundance. However, a negative correlation between chlorophyll concentration in April and bottlenose whale density across the broader northeast Atlantic over summer periods from 1998 to 2015 was also identified by Ramírez-Martínez and Hammond (2019, their figure 25). The result may be explained by the incorporation of the two-month temporal lag, which might not be effective in capturing the spatial disconnect between surface productivity and deep-water prey abundance, and/or the effect of

406 chlorophyll concentration on prey abundance. Alternatively, there could potentially be other unexplored
407 environmental variable(s) which would better explain the observed negative relationship ecologically. We
408 suggest future study to obtain field data with longer temporal coverage and further explore the effect of
409 other environmental variables on bottlenose whale occurrence or density.

410 The Poisson GAM showed that depth-slope interactions and whale distance from the Arctic front were
411 significant predictors of additional whale sightings given first encounter. However, distance from the
412 Arctic front did not gain statistical support when it was specified in the zero-inflated Poisson GAM,
413 indicating that the effect identified in the Poisson GAM was not robust. More whale sightings at water
414 depths between 1,000 m and 2,500 m (Fig. 5a) was consistent with findings in the literature; bottlenose
415 whales in the Gully and northeast Atlantic waters are mainly found in offshore waters deeper than 500 m
416 (Benjaminsen 1972, Benjaminsen & Christensen 1979, Hooker 1999, Taylor et al. 2008, Rogan et al.
417 2017, Ramírez-Martínez et al. 2020). Reliance on submarine canyons by the Gully population might even
418 cause it to be genetically different from individuals from the rest of eastern Canada (Feyrer, 2021), as
419 whales around the Labrador-Davis Strait are more evenly distributed along the continental shelf edge and
420 in deep basins (Reeves et al.1993, Gomez et al. 2017, Feyrer 2021). Preference for deeper water could
421 be driven by the downward vertical migration in maturing prey *Gonatus* (Hooker, 1999, Bjørke 2001).
422 Although some whales were sighted at shallower water depths (<500 m) in the field, predicted effect of
423 interaction term between mean depth and slope revealed that steep seafloor topography (and thus deeper
424 water) was located nearby.

425 Despite the unclear effect of seasonal migration (Benjaminsen & Christensen 1979, Reeves et al. 1993)
426 on the habitat use of bottlenose whales in the northeast Atlantic, the potential migration patterns might
427 be one of the reasons resulting in low percentages of deviance explained by the best models of sighting
428 occurrence and additional whale sightings given first encounter in this study. Whaling records in Norway
429 suggested that bottlenose whales might reach their northern distribution in spring and early summer, and
430 migrate southward in by July (Reeves et al. 1993). The north-south migration hypothesis is further

supported by Miller et al (2015b) who tagged whales off the Jan Mayen Island in June 2015. The tagged individuals exhibited southward directional movements, with one travelling long distances to the Azores Archipelago between late June and early August in 2015. Whale strandings along Europe and Ireland, peaking in late summer and autumn, suggested northward whale movement in spring and later southward movement between late summer and autumn (Whitehead & Hooker 2012). Year-round records of bottlenose whales off the Faroe Islands (Bloch et al. 1996) and Norway (Øien & Hartvedt 2011) suggest that bottlenose whales in the northeast North Atlantic might exhibit inshore-offshore movement driven by the seasonal change of prey abundance (Whitehead & Hooker 2012). In this study some whale sightings were recorded during the vessel transit between Jan Mayen Island and Iceland (Fig. 1), which could have been of whales on their way migrating southward or offshore.

5.1.2 Spatial Prediction of Whale Habitat Use Over the Wider Prediction Area

Spatial predictions of whale habitat use over a wider area using the two-model approach (Fig. 6) corresponded to field observations of this study: *in-situ* bottlenose whale sightings were mostly made to the east of Jan Mayen Island and submarine canyon southeast of Jan Mayen. They also indicated that the submarine canyon area to the southeast of Jan Mayen Island (marine region ranging from 70.8° N and 6.5° W, to 71.2° N and 5.5° W) could be a high-use site by bottlenose whales in summer. These estimates were largely consistent with the model predictions of both the binomial and Poisson GAMs of this study, and average density prediction for bottlenose whales from 1998 to 2005 for the broader northeast North Atlantic by Ramírez-Martínez and Hammond (2019, see their Fig. 26).

Apparent preference for submarine canyon habitats has been observed in bottlenose whales, sperm whales and striped dolphins (*Stenella coeruleoalba*) in the Gully off Nova Scotia, and sperm whales within the Andøya Canyon northwest of Andenes, Norway (Teloni, et al. 2008). Submarine canyons are often regarded as biomass and biodiversity hotspots (Vetter & Dayton 1999, De Leo et al. 2010, Amaro et al. 2016), which are capable to sustain ecologically complex communities. These topographic features act as the conduits for the influx of macrophyte detritus and diel vertical migrators which are later distributed

456 throughout much of the canyon system by strong gravity currents (Greene et al. 1988, Vetter & Dayton
457 1999). Canyon hydrographic effects such as accelerated currents enhance the concentration of suspended
458 particulate matter (De Leo et al.2010). Organic matter together with strong habitat heterogeneity within
459 canyons substantially support a diversity and abundance of benthic fauna, including mega-benthic
460 invertebrates (De Leo et al. 2010, Santo 2010) and deep-sea fish (Vetter & Dayton 1999). Epibenthic
461 diversity within the Jan Mayen Fracture zone (and the submarine canyon) is relatively high, in which
462 Oschmann (1991) identified 36 taxa and Santo (2010) found 47 identifiable species among 66 disparate
463 species (including crinoidean, anthozoan, tunicate, poriferan, fishes, and hexacorallia corals). The
464 eurybathic species appears to be remarkably abundant between 580 m and 3,222 m (Oschmann 1991).
465 This might favour the underwater aggregation of adult *Gonatus* squid at 1,000 m or below or other prey
466 and in turn attract bottlenose whales to forage within the canyon area.

467 Although higher sighting rates were also estimated in waters from 71.3° N and 4.5° W, to 71.8° N and
468 1.5° W, northern and northwestern waters off the Jan Mayen Island, as well as waters on south of the
469 study region (similar southern Jan Mayen pattern was also predicted by Ramírez-Martínez and Hammond
470 (2019), model estimates of these areas should be treated carefully as at-field whale observations or
471 dedicated survey effort did not cover these areas.

472 In addition, the two-model approach alias hurdle model can only deal with excessive zeros by modelling
473 additional whale sightings given first encounter with zero-truncated Poisson distribution, but not
474 differentiating true zeros (i.e., actual absence of an animals) from false zeros (i.e., animal is present but
475 detected). As some false zeros might potentially arise from availability or perception bias, these model
476 predictions should therefore be corroborated by systematic and ideally year-round line-transect study
477 incorporating both visual and acoustic detection. Such monitoring would help to equally sample the whole
478 survey area, while survey bias on detection probability can be minimized. By reducing false zeros and
479 model prediction uncertainty, this can potentially inform the delineation of marine protected area(s)

(MPAs) covering important whale habitat in Jan Mayen waters for effective conservation of bottlenose whales in the northeast North Atlantic.

5.2 Conservation Insights of Northern Bottlenose Whales off Jan Mayen Island

Our study indicates a potential key habitat for northern bottlenose whales around Jan Mayen in June, particularly the submarine canyon area to the southeast of the island. This potential high-use site is not under any statutory protection currently, such as the Jan Mayen Nature Reserve designated in 2010 covering a total area of 4,315 km^2 of Jan Mayen territorial waters (up to 22.2 km from the island, Bruserud et al. 2010).

In the meantime, oil and gas surveys using airguns have been frequent along the coast of Norway (see www.npd.no/en/). The Norwegian government recently proposed to open its waters to deep-sea mining (see https://www.reuters.com/sustainability/climate-energy/norway-moves-open-its-waters-deep-sea-mining-2023-06-20/). Recent study documented the effects of airgun sounds to narwhals (*Monodon monoceros*) (Heide-Jørgensen et al. 2021), another marine mammal species living in high-latitude regions. Though northern bottlenose whales can display strong inquisitiveness to unfamiliar sounds (Hooker 1999, Miller et al. 2015), acoustic disturbance is regarded as one of the key threats to this beaked whale species (Whitehead et al. 2021). Beaked whales may be more behaviourally responsive to manmade noise in relatively pristine waters such as around the Jan Mayen compared to areas with frequent human activity (Wensveen et al. 2019). Northern bottlenose whales were found to exhibit strong behavioural responses with relatively low response thresholds to sonar signals, with long-term area avoidance and cessation of echolocation-based foraging (Miller et al. 2015, Sivle et al. 2015, Wensveen et al. 2019), indicating consequent risk from marine development and naval activity. Along with these previous research, study findings here can, to a certain extent, inform management of underwater noise threats by minimizing spatial overlap between potential high-use areas of bottlenose whales and future noise-generating anthropogenic activities, such as seismic surveys.

6. Acknowledgements

We would like to express our sincere gratitude to everyone involved in the Jan Mayen fieldwork, including Captains Christian Harboe-Hansen and Chris Rose and the rest of the ship's crews. Thanks to the science crews including Tomoko Narazaki, Kagari Aoki, Leigh Hickmott, Lucia Martina Martin Lopez, Lars Kleivane, Rune Hansen, Miguel Neves dos Reis, Dr. Eilidh Siegal, Paul Wensveen, Eva Hartvig, Mike Williamson, Naomi Boon, Joanna Kershaw, Hannah Wood, Eva Hartvig, and Charlotte Curé. Invaluable scientific and/or editorial advice was provided by Prof. Phil Hammond, Nadya Ramirez-Martinez, Guilherme Augusto Bortolotto, the editor and anonymous reviewers to improve the quality of this manuscript. The project was primarily funded by SERDP project RC-2337 and the US Office of Naval Research.

7. Literature Cited

513 Agarwal DK, Gelfand AE & Citron-Pousty S (2002) Zero-inflated models with application to spatial count
514 data. Environmental and Ecological Statistics 9(4): 341–355
515 Akaike H (1992) Information Theory and an Extension of the Maximum Likelihood. Springer-Berlag,
516 New York
517 Amaro T, Huvenne VAI, Allcock AL, Aslam T, Davies JS, Danovaro R, De Stigter HC, Duineveld GCA,
518 Gambi C, Gooday AJ, Gunton LM, Hall R, Howell KL, Ingels J, Kiriakoulakis K, Kershaw CE,
519 Lavaleye MSS, Robert K, Stewart H, Van Rooij D, White M, Wilson AM (2016) The Whittard
520 Canyon – A case study of submarine canyon processes. Progress in Oceanography 146:38–57
521 Barry SC & Welsh AH (2002) Generalized additive modelling and zero inflated count data. Ecological
522 Modelling, 157, 179–188
523 Barton K (2015) MuMin: multi-model inference. R package, version 1.15.6. r-forge.r-
524 project.org/projects/mumin/(accessed 25 Jan 2017)
525 Benjaminsen T (1972) On the biology of the bottlenose whale, *Hyperoodon ampullatus* (Forster).
526 Norwegian Journal of Zoology 20:233–241
527 Benjaminsen T, Christensen I (1979) The natural history of bottlenose whales, *Hyperoodon ampullatus*. In:
528 Behaviour of marine mammals: current perspectives in research (pp. 143–164). Plenum Press, New
529 York.
530 Bjøke H (2001) Predators of the squid *Gonatus fabricii* (Lichtenstein) in the Norwegian Sea. Fisheries
531 Research 52:113–120
532 Bjørke H (1995) Norwegian investigations on *Gonatus fabricii* (Lichtenstein).
533 hdl.handle.net/11250/105443 (accessed 25 Jan 2017)
534 Blasco-Moreno A, Pérez-Casany M, Puig P, Morante M, & Castells E (2019) What does a zero mean?
535 Understanding false, random and structural zeros in ecology. Methods in Ecology and Evolution
536 10(7):949–959
537 Bloch D, Desportes G, Zachariassen M & Christensen I (1996) The northern bottlenose whale in the Faroe

538 Islands, 1584-1993. Journal of Zoology 239(1):123–140
539 Børsheim KY, Milutinovi S, Drinkwater KF (2014) TOC and satellite-sensed chlorophyll and primary
540 production at the Arctic Front in the Nordic Seas. Journal of Marine Systems 139:373–382
541 Bruserud H, Grimstad K, Høyland TK, Stokkan BE, Egeland LC (2010) Forskrift om fredning av Jan
542 Mayen naturreservat. lovdata.no/dokument/SF/forskrift/2010-11-19-1456 (accessed 4 Nov 2019)
543 Buckland ST, Anderson DR, Burnham KP, Borchers DL, Thomas L (2004) Advanced Distance Sampling:
544 Estimating abundance of biological populations. Oxford University Press, Oxford
545 Buckland ST, Anderson DR, Burnham KP, Laake JL, Borchers DL, Thomas L (2001) Introduction to
546 Distance Sampling: Estimating abundance of biological populations. Oxford University Press,
547 Oxford.
548 Burnham KP, Anderson DR (2002) Model Selection and Multimodel Inference: A Practical Information-
549 Theoretic Approach. Springer New York, New York
550 Cañadas A, Sagarminaga R, De Stephanis R, Urquiola E, Hammond PS (2005) Habitat preference
551 modelling as a conservation tool: Proposals for marine protected areas for cetaceans in southern
552 Spanish waters. Aquatic Conservation: Marine and Freshwater Ecosystems 15(5):495–521
553 Cavanaugh JE (1997) Unifying the Derivations for the Akaike and Corrected Akaike Information Criteria.
554 Statistics and Probability Letters 33:201–208
555 Chen C (2000) Generalized additive mixed models. Communications in Statistics - Theory and Methods
556 29(5–6):1257–1271
557 Compton RC (2004) Predicting key habitat and potential distribution of northern bottlenose whales
558 (*Hyperoodon ampullatus*) in the northwest Atlantic Ocean. MSc dissertation, Unniveristy of Plymouth,
559 Plymouth
560 COSEWIC (2011) COSEWIC Assessment and Status Report on the Northern Bottlenose Whale
561 Hyperoodon ampullatusin Canada. Committee on the Status of Endangered Wildlife in Canada.
562 Ottawa.

563 Cragg JG (1971) Some Statistical Models for Limited Dependent Variables with Application to the
564 Demand for Durable Goods. Econometrica 39(5): 829–844
565 Cramér H (1928) On the Composition of Elementary Errors. Scandinavian Actuarial Journal 1:13–74
566 de Greef E, Einfeldt AL, Miller PJO, Ferguson SH, Garroway CJ, Lefort KJ, Paterson IG, Bentzen P,
567 Feyrer LJ (2022) Genomics reveal population structure, evolutionary history, and signatures of
568 selection in the northern bottlenose whale, *Hyperoodon ampullatus.* Molecular Ecology
569 31(19):4919–4931
570 De Leo FC, Smith CR, Rowden AA, Bowden DA, Clark MR (2010) Submarine canyons: hotspots of
571 benthic biomass and productivity in the deep sea. Proceedings of the Royal Society B: Biological
572 Sciences 277(1695):2783–2792
573 Durbin J, Watson GS (1971) Testing for serial correlation in least squares regression. III. Biometrika 58(1):
574 1–19
575 Einfeldt A, Feyrer LJ, Paterson I, Ferguson S, Miller P, de Greef E & Bentzen P (2022) Characterization
576 of Population Structure in Northern Bottlenose Whales (*Hyperoodon ampullatus*) in the North
577 Atlantic from an Analysis of Microsatellite Data - Canadian Technical Report of Fisheries and
578 Aquatic Sciences 3467
579 Embling CB, Gillibrand PA, Gordon J, Shrimpton J, Stevick PT, Hammond PS (2010) Using habitat
580 models to identify suitable sites for marine protected areas for harbour porpoises (*Phocoena phocoena*).
581 Biological Conservation 143(2):267–279
582 Eppley RW (1972) Temperature and phytoplankton growth in the sea. Fishery Bulletin 70(4):1063–1085
583 Erga SR, Ssebiyonga N, Hamre B, Frette O, Hovland E, Hancke K, Drinkwater KF, Rey F (2012)
584 Environmental control of phytoplankton distribution and photosynthetic performance at the Jan
585 Mayen Front in the Norwegian Sea. Journal of Marine Systems 130:193-205.
586 Fernández R, Pierce GJ, MacLeod CD, Brownlow A, Reid RJ, Rogan E, Addink M, Deaville R,
587 Jepson PD, Santos MB (2014) Strandings of northern bottlenose whales, *Hyperoodon ampullatus*, in

588 the north-east Atlantic: Seasonality and diet. Journal of the Marine Biological Association of the
589 United Kingdom 94(6):1109–1116
590 Feyrer LJ (2021) Northern Bottlenose Whales in Canada: The Story of Exploitation, Conservation and
591 Recovery. PhD Dissertation. Dalhousie University, Halifax, NS
592 Feyrer LJ, Zhao ST, Whitehead H, Matthews CJD (2020) Prolonged maternal investment in northern
593 bottlenose whales alters our understanding of beaked whale reproductive life history. PLoS ONE
594 15:1–19
595 Forney KA (2000) Environmental Models of Cetacean Abundance : Reducing Uncertainty in Population
596 Trends. Conservation Biology 14(5):1271–1286
597 Fox J, Weisberg S, Adler D, Bates D, Baud-bovy G, Ellison S, Firth D, Friendly M, Gorjanc G, Graves S,
598 Heiberger R, Laboissiere R, Monette G, Murdoch D, Nilsson H, Ogle D, Ripley B, Venables W,
599 Winsemius D, Zeileis A (2016) Package 'car.' r-forge.r-project.org/projects/car/ (accessed 27 Jan
600 2017)
601 Glennie R, Buckland ST, Thomas L (2015) The Effect of Animal Movement on Line Transect Estimates
602 of Abundance. PLoS ONE 10(3): e0121333
603 Global Radiation Group. (2017). NOAA Solar Calculator. Retrieved from
604 https://www.esrl.noaa.gov/gmd/grad/solcalc/
605 Gomez C, Lawson J, Kouwenberg AL, Moors-Murphy H, Buren A, Fuentes-Yaco C, Marotte E,
606 Wiersma YF, Wimmer, T (2017) Predicted distribution of whales at risk: Identifying priority areas
607 to enhance cetacean monitoring in the Northwest Atlantic Ocean. Endangered Species Research
608 32(1):437–458
609 Gowans S, Whitehead HAL, Hooker SK (2001) Social organization in northern bottlenose whales,
610 *Hyperoodon ampullatus* : not driven by deep-water foraging ? Animal Behaviour 62:369–377
611 Gowans S, Whitehead H, Arch JK, Hooker SK (2000) Population size and residency patterns of northern
612 bottlenose whales (*Hyperoodon ampullatus*) using the Gully, Nova Scotia Population size and residency

patterns of northern bottlenose whales (*Hyperoodon ampullatus*) using the Gully, Nova Scotia. Journal of Cetacean Research and Management 2(3):201–210

Greene ACH, Wiebe PH, Burczynski J, Youngbluth MJ (1988) Acoustical Detection of High-Density Krill Demersal Layers in the Submarine Canyons off Georges Bank. Science 241(4863):359–361

Guisan A, Zimmermann NE (2000) Predictive habitat distribution models in ecology. Ecological Modelling 135:147–186

Hammond PS, Berggren P, Benke H, Borchers DL, Collet A, Heide-Jørgensen MP, Heimlich S, Hiby A R, Leopold MF, Øien N (2002) Abundance of harbour porpoise and other cetaceans in the North Sea and adjacent waters. Journal of Applied Ecology 39:361–376

Hammond PS, Macleod K, Gillespie D, Swift R, Winship A, Burt ML, Cañadas A, Vazquez JA, Ridoux V, Certain G, Van Canneyt O, Lens S, Santos S, Rogan E, Uriarte A, Hernandez C, Castro R, (2009) Cetacean Offshore Distribution and Abundance in the European Atlantic. Final Report (CODA). University of St. Andrews, St Andrews

Hammond PS, Macleod K, Berggren P, Borchers DL, Burt L, Cañadas A., Desportes G, Donovan GP, Gilles A, Gillespie D, Gordon J, Hiby L, Kuklik I, Leaper R, Lehnert K, Leopold M, Lovell P, Øien N, Paxton CGM, Ridoux V, Rogan E, Samarra F, Scheidat M, Sequeira M, Siebert U, Skov H, Swift R, Tasker ML, Teilmann J, Canneyt OV, Antonio J (2013) Cetacean abundance and distribution in European Atlantic shelf waters to inform conservation and management. Biological Conservation 164:107–122

Hastie T, Tibshirani R (1986) Generalized Additive Models. Statistical Science 1(3):297-318

Hátún H, Payne MR, Beaugrand G, Reid PC, Sandø AB, Drange H, Hansen B, Jacobsen JA, Bloch D (2009) Large bio-geographical shifts in the north-eastern Atlantic Ocean: From the subpolar gyre, via plankton, to blue whiting and pilot whales. Progress in Oceanography 80(3–4):149–162

Hedley S, Buckland ST, Borchers D (1999) Spatial modeling from line transect data. Journal of Cetacean Research and Management 1(3)

638 Heide-Jørgensen MP, Blackwell SB, Tervo OM, Samson AL, Garde E, Hansen RG, Ngô MC, Conrad AS,
639 Trinhammer P, Schmidt HC, Sinding MHS, Williams TM, Ditlevsen S (2021) Behavioral Response
640 Study on Seismic Airgun and Vessel Exposures in Narwhals. Frontiers in Marine Science 8:1–23
641 Hooker SK, Whitehead H, Gowans S (1999) Marine protected area design and the spatial and temporal
642 distribution of cetaceans in a submarine canyon. Conservation Biolog 13(3):592–602
643 Hooker SK (1999) Resource and habitat use of northern bottlenose whales in the Gully : ecology , diving
644 and ranging behaviour. PhD Dissertation. Dalhousie University, Halifax, NS
645 Hooker SK, Baird RW (1999) Deep-diving behaviour of the northern bottlenose whale, *Hyperoodon*
646 *ampullatus* (Cetacea : Ziphiidae). Proceedings of the Royal Society 266:671–676
647 Hooker SK, Iverson SJ, Ostrom P, Smith SC (2001) Diet of northern bottlenose whales inferred from
648 fatty-acid and stable-isotope analyses of biopsy samples Diet of northern bottlenose whales inferred
649 from fatty-acid and stable-isotope analyses of biopsy samples. Canadian Journal of Zoology 79:1442–
650 1454
651 Hooker SK, Whitehead H, Gowans S, Baird RW (2002) Fluctuations in distribution and patterns of
652 individual range use of northern bottlenose whales. Marine Ecology Progress Series 225:287–297
653 IHO-IOC (2017) IHO-IOC GEBCO Gazetteer of Undersea Feature Names. www.gebco.net (accessed 7
654 Aug 2017)
655 IMBER IPO (2012) IMBER Issue n°21 - September 2012.
656 www.imber.info/Products/Newsletters/Issue-n-21-September-2012 (accessed 7 Aug 2017)
657 IOC IHO, BODC (2003) Centenary Edition of the GEBCO Digital Atlas.
658 www.gebco.net/data_and_products/gridded_bathymetry_data/ (accessed 7 Aug 2017)
659 Isojunno S, Matthiopoulos J, Evans PGH (2012) Harbour porpoise habitat preferences : robust spatio-
660 temporal inferences from opportunistic data. Marine Ecology Progress Series 448:155–170
661 Kastelein RA, Gerrits NM (1991) Swimming, diving, and respiration patterns of a Northern bottlenose
662 whale (*Hyperoodon ampullatus*, Forster, 1770). Aquatic Mammals 17(1):20–30

663 Kenny RD, Payne PM, Heinemann D, Winn HE (1996) Shifts in Northeast shelf cetacean distributions
664 relative to trends in Gulf of Maine / Georges Bank finfish abundance. In: Sherman K, Jaworski NA,
665 Smayda T (eds) The Northeast Shelf Ecosystem: Assessment, Sustainability, and Management.
666 Blackwell Science, Cambridge
667 Krausma, PR (1999) Some Basic Principles of Habitat Use. In: Launchbaugh KL, Sanders KD, Mosley JL
668 (eds) Grazing Behaviour of Livestock and Wildlife. Idaho Forest, Wildlife and Range Experiment
669 Statation Bulletin No. 70, University of Idaho, Moscow, ID
670 Lick B, Piatkowski U (1998) Stomach Contents of a Northern Bottlenose Whale (*Hyperoodon Ampullatus*)
671 Stranded at Hiddensee, Baltic Sea. Journal of the Marine Biological Association of the United
672 Kingdom 78(2):643-650
673 Marques FFC, Buckland ST (2003) Incorporating Covariates into Standard Line Transect Analyses.
674 Biometrics 59:924–935
675 Marshall ML, David A, Miller L (2016) Package ' Distance .' cran.r-
676 project.org/web/packages/Distance/Distance.pdf (accessed 27 Jan 2017)
677 Mellin C, Russell BD, Connell SD, Brook BW & Fordham DA (2012) Geographic range determinants of
678 two commercially important marine molluscs. Diversity and Distributions 18(2): 133–146
679 Michalsky J (1988) The Astronomical Almanac's algorithm for approximate solar position (1950-2050).
680 Solar Energy 40(3):227–235
681 Miller PJO, Kvadsheim PH, Lam FPA, Tyack PL, Curé C, Deruiter SL, Kleivane L, Sivle LD, Ijsselmuide,
682 SPV, Visser F, Wensveen PJ, Benda-Beckmann AM, Martín López LM, Nrazaki T, Hooker SK
683 (2015) First indications that northern bottlenose whales are sensitive to behavioural disturbance
684 from anthropogenic noise. Royal Society Open Science 2:140484
685 Miller PJO, Narazaki T, Isojunno S, Hansen R, Kershaw J, Neves dos Reis M, Kleivane L (2015) Body
686 condition and 3S15 projects: 2015 Jan Mayen trial. Internal SMRU report available by email from
687 pm29@st-andrews.ac.uk

688 Miller PJO, Wensveen PJ, Isojunno S, Hansen R, Neves dos Reis M, Kleivane L (2014) Body condition
689 project 2014 Jan Mayen Trial. Internal SMRU report available by email from pm29@st-
690 andrews.ac.uk
691 Miller PJO, Wensveen PJ, Isojunno S, Hansen R, Neves dos Reis M, Kleivane L (2016) 3S3 and body
692 condition projects : 2016 Jan Mayen 2016 trial. Internal SMRU report available by email from
693 pm29@st-andrews.ac.uk
694 NAMMCO (1995) Report of the Third Meeting of the Scientific Committee. In: NAMMCO Annual
695 Report 1995, NAMMCO, Tromsø, Norway
696 Øien N & Hartvedt S (2011) Northern bottlenose whales *Hyperoodon ampullatus i*n Norwegian and
697 adjacent waters. International Whaling Commission, IWC SC/63/SM1. Cambridge
698 Oschmann W (1991) Ecology and Bathymetry of the Late Quaternary Shelly Macribenthos from Bathyal
699 and Abyssal Areas of the Norwegian Sea. Senckenbergiana Maritima 21:155–189
700 Piechura J, Walczowski W (1995) The Arctic Front : structure and dynamics. Oceanologia 37(1):47–73
701 Potts JM & Elith J (2006) Comparing species abundance models. Ecological Modelling 199(2):153–163
702 R Core Team (2017) R: A language and environment for statistical computing. R Foundation for Statistical
703 Computing. www.r-project.org/ (accessed 7 Aug 2017)
704 Raj RP, Chatterjee S, Bertino L, Turiel A & Portabella M (2019) The Arctic Front and its variability in
705 the Norwegian Sea. Ocean Science 15(6): 1729–1744
706 Ramírez-Martínez NC, Hammond PS (2019) Distribution and habitat use of deep-diving cetaceans in the
707 central and north-eastern north Atlantic, NAMMCO Scientific Committee Abundance Estimation
708 Working Group Document SC/26/AEWG/15.
709 Redfern JV, Barlow J, Bailance LT, Gerrodette T, Becker EA (2008) Absence of scale dependence in
710 dolphin-habitat models for the eastern tropical Pacific Ocean. Marine Ecology Progress Series, 363,
711 1–14. https://doi.org/10.3354/meps07495
712 Redfern JV, Ferguson MC, Becker EA, Hyrenbach KD, Good C, Barlow J, Kaschner K, Baumgartner MF,

713 Forney KA, Ballance LT, Fauchald P, Halpin P, Hamazaki T, Pershing AJ, Qian SS, Read A, Reilly
714 SB, Torres L, Werner F (2006) Techniques for cetacean - habitat modeling. Marine Ecology
715 Progress Series 310:271–295
716 Reeves RR, Mitchell E, Whitehead H (1993) Status of the northern bottlenose whale, *Hyperoodon*
717 *ampullatus*. Canadian Field-Naturalist 107:490–508
718 Rogan E, Cañadas A, Macleod K, Santos B, Mikkelsen B, Uriarte A, Canneyt OV, Vázquez JA, Hammond
719 PS (2017). Distribution, abundance and habitat use of deep diving cetaceans in the North-East
720 Atlantic. Deep-Sea Research Part II 141:8-19
721 Santo E (2010) Community analysis of large epibenthos in the Nordic Seas. MSc dissertation. University
722 of Iceland, Reykjavik, Iceland
723 Schepper SD, Schreck M, Beck KM, Matthiessen J, Fahl K (2015) Early Pliocene onset of modern Nordic
724 Seas circulation related to ocean gateway changes. Nature Communications 6:8659
725 Shadish WR, Zuur AF, Sullivan KJ (2014) Using generalized additive (mixed) models to analyze single
726 case designs. Journal of School Psychology 52(2):149–178
727 Sivle LD, Kvadsheim PH, Curé C, Isojunno S, Wensveen PJ, Lam F A, Visser F, Kleivane L, Tyack PL,
728 Harris CM, Miller PJO (2015) Severity of Expert-Identified Behavioural Responses of Humpback
729 Whale, Mike Whale, and Northern Bottlenose Whale to Naval Sonar. Aquatic Mammal 41(4):469–
730 502
731 Skagseth Ø, Broms C, Gundersen K, Hátún H, Kristiansen I, Larsen KMH, Mork KA, Petursdottir H,
732 Søiland H (2022) Arctic and Atlantic Waters in the Norwegian Basin, Between Year Variability and
733 Potential Ecosystem Implications. Frontiers in Marine Science 9(May): 1–14
734 Smith A, Hofner B, Lamb JS, Osenkowski J, Allison T, Sadoti G, McWilliams SR, Paton P (2019)
735 Modeling spatiotemporal abundance of mobile wildlife in highly variable environments using
736 boosted GAMLSS hurdle models. Ecology and Evolution 9(5): 2346–2364
737 Smith RC, Dustan P, Au D, Baker KS, Dunlap EA (1986). Distribution of cetaceans and sea-surface

chlorophyll concentrations in the California Current. Marine Biology 91:385–402

Storrie L, Lydersen C, Andersen M, Wynn RB, Kovacs KM (2018) Determining the species assemblage and habitat use of cetaceans in the Svalbard Archipelago, based on observations from 2002 to 2014. Polar Research 37(1)

Taylor BL, Baird R, Dawson SM, Ford J, Mead JG, Sciara NG, Wade P, Pitman RL (2008) *Hyperoodon ampullatus* , North Atlantic Bottlenose Whale. dx.doi.org/10.2305/IUCN.UK.2008.RLTS.T10707A3208523.en (accessed 7 Aug 2017)

Teloni V, Mark JP, Patrick MJO, Peter MT (2008) Shallow food for deep divers: Dynamic foraging behavior of male sperm whales in a high latitude habitat. Journal of Experimental Marine Biology and Ecology 354(1):119–131

Thomas R, Lello J, Medeiros R, Pollard A, Seward A, Smith J, Vafidis J, Vaughan I (2015) Data analysis with R statistical software - A guidebook for scientists. Eco-explore, Cardiff

Vetter EW, Dayton PK (1999) Organic enrichment by macrophyte detritus, and abundance patterns of megafaunal populations in submarine canyons. Marine Ecology Progress Series 186:137–148

Vuong QH (1989) Likelihood ratio tests for model selection and non-nested hypotheses. Econometrica 57:307–333

Waring GT, Hamazaki T, Sheehan D, Wood G, Baker S (2001) Characterization of beaked whale (Ziphiidae) and sperm whale (*Physeter marocephalus*) summer habitat in shel-edge and deeper waters off the Northwast U.S. Marine Mammal Science 17(4):703–717

Wensveen PJ, Isojunno S, Hansen RR, Benda-beckmann AMV, Kleivane L, Ijsselmuide SV, Lam FA, Kvadsheim PH, Deruiter SL, Curé C, Narazaki T, Tyack PL, Miller PJO (2019) Northern bottlenose whales in a pristine environment respond strongly to close and distant navy sonar signals. Proceedings of the Royal Society B: Biological Sciences 286:20182592

761 Whitehead H, Reeves R, Feyrer L, Brownell JRL (2021) *Hyperoodon ampullatus.* The IUCN Red List of
762 Threatened Species 2021. dx.doi.org/10.2305/IUCN.UK.2021-1.RLTS.T10707A50357742.en
763 (accessed 10 Oct 2021)

764 Whitehead H, Faucher A, Gowans S, McCarrey S (1997) Status of the Northern Bottlenose Whale,
765 *Hyperoodon ampullatus*, in the Gully, Nova Scotia. Canadian Field-Naturalist 111:287-292

766 Whitehead H, Hooker SK (2012) Uncertain status of the northern bottlenose whale *Hyperoodon ampullatus* :
767 population fragmentation , legacy of whaling and current threats. Endangered Species Research
768 19:47–61

769 Wiborg KF, Gjøsater J, Beck IM (1982) The squid *Gonatus fabricii* (Lichetenstein): Investigations in the
770 Norwegian Sea and western Barents Sea 1978-1981. ICES, Copenhagen, Denmark

771 Wood S (2016) Package 'mgcv.' cran.r-project.org/web/packages/mgcv/mgcv.pdf (accessed 25 Jan
772 2017)

773 Wood SN (2006). Generalized Additive Models: An Introduction with R. CRC Press, New York

774 Zuur AF, Ieno EN, Walker NJ, Saveliev AA & Smith GM (2009) Zero-Truncated and Zero-Inflated
775 Models for Count Data. In Mixed effects models and extensions in ecology with R (pp. 261–293).
776 New York, Springer New York

777

778 # Tables

779 **Table 1|Selected survey effort and whale sightings by year**

	2014	2015	2016	Total
Start date of survey	10 June	15 June	02 June	-
End date of survey	26 June	02 July	24 June	-
Research vessel and length	T/S PROLIFIC (29 m)	Donna Wood (32 m)	Donna Wood	-
Survey duration (h)	166.0	152.4	201.1	519.5 h
Distance surveyed (km)	1237.4	1137.4	1574.9	3949.7
Number of sightings	77	75	68	220
Average group size of whale sightings	3.01 (± 1.11)	3.08 (± 1.59)	3.19 (± 1.59)	3.09 (± 1.44)
Number of 12.5km effort segments	99	91	126	316
Number of segments with sightings	46	31	37	114

780

781 **Table 2| Predictor variables for habitat models of sighting presence and additional whale sightings given first encounter**

Variable	Spatial Resolution	Temporal Resolution	Description	Data Source
Static predictor variables				
depth.m	30arc-sec	N/A	Average water depth in metres (m)	Gridded bathymetry data from General Bathymetric Chart of the Oceans (GEBCO), obtained from interpolated depth soundings from ship (IOC, IHO and BODC, 2003)
slope.max			Maximum degree of seafloor inclination from the horizontal surface, angle in degree (°)	Derived from GEBCO gridded bathymetry data
aspect			Average seafloor orientation in which the slope is facing, in number degrees of east (°) increasing counter clockwise	

distAF	N/A		Distance from the Arctic front in kilometres (km)	Steady distance values calculated based on the location of Arctic front illustrated by Piechura & Walczowski (1995), IMBER IPO (2012) and Børsheim et al. (2014).
dist2000			Distance from the nearest 2,000m contour, in kilometres (km). Positive value for sample point located at water depth ≥ 2,000m, and negative value for point at water depth < 2,000m	Derived from GEBCO gridded bathymetry data
Dynamic predictor variables				
Chla	1 x 1km	Monthly averaged (April)	Average sea surface chlorophyll *a* concentration in 2014 to 2016, in milligram m-^{3} (mg m^{-3})	Monthly-mean satellite data of global ocean chlorophyll (global colour processor) provided by the E.U. Copernicus Marine Service Information
SST	0.25 x 0.25 degree		Average sea surface temperature in 2014 to 2016, in Kelvin (K).	Daily-mean *in situ* and satellite ensemble products of global ocean sea surface temperature from 11 analysis systems. Data obtained from the E.U. Copernicus Marine Service Information
SSH	0.083 x 0.083 degree		Average sea surface height in metres(m) above geoid in 2014 to 2016	Daily-mean numerical-model data of sea surface height assimilated using the Incremental Analysis Update (IAU) method. Data obtained from the E.U. Copernicus Marine Service Information
SA		Monthly averaged (June)	Average sea surface salinity in 2014 to 2016, in 1e^{-3}	Daily-mean numerical-model data of salinity assimilated using the Incremental Analysis Update (IAU) method. Advection of the salinity tracers was computed with the total variance diminishing (TVD) advection scheme. Data obtained from the E.U. Copernicus Marine Service Information
Temporal predictor variables				
solar elevation	N/A	Hourly	Solar position in terms of sun elevation angle measured up from the horizon, in degree (°)	Calculated based on the algorithm provided by Michalsky (1988)
year		Yearly	Survey year	*In situ* data

782

783

Table 3| Summary information for detection function models. Models are sorted in ascending order of AIC. hr.model was the final best model. hr: hazard-rate key function, hn: half-normal key function, CV: coefficient of variation.

	Key function	Formula	AIC	Cramer-von Mises p-value	Average detectability	Standard Error	CV	ΔAIC
hr.model	hr	~1	2088	0.79	0.326	0.047	0.15	0
hr.n.model	hr	~as.factor(grouped_size)	2094.3	0.84	0.336	0.048	0.14	6.3
hr.ss.model	hr	~as.factor(grouped_beaufort)	2094.6	0.88	0.305	0.048	0.16	6.6
hr.ss.n.model	hr	~as.factor(grouped_beaufort) + as.factor(grouped_size)	2100.7	0.91	0.316	0.048	0.15	12.7
hn.model	hn	~1	2114.7	0	0.51	0.025	0.05	26.7

Table 4| Summary of the best models of sighting occurrence and number of additional sightings, given first encounter. MaxK: maximum number of knots allowed, edf: estimated degree of freedom, %DevEx: % deviance explained

	Covariates	MaxK	edf	p-value (α = 0.05)	%DevEx	UBRE	AIC	Model Weight
Best sighting occurrence model	slope.max	4	0.798	0.038	8.44	0.2438	393.1	0.03
	April Chla	4	1.84	0.028				
	August SST	4	2.902	0.010				
	depth.m:slope.max	5	0.807	0.178				
Best additional sightings model	depth.m:slope.max	8	3.68	0.001	23.4	0.1899	258.129	0.036
	distAF	4	2.15	0.015				
	April Chla	6	1.93	0.111				
	August SST	5	0	0.472				
	depth.m	4	0	0.704				
	slope.max	6	0	0.895				
	aspect	6	0	0.944				

Figures

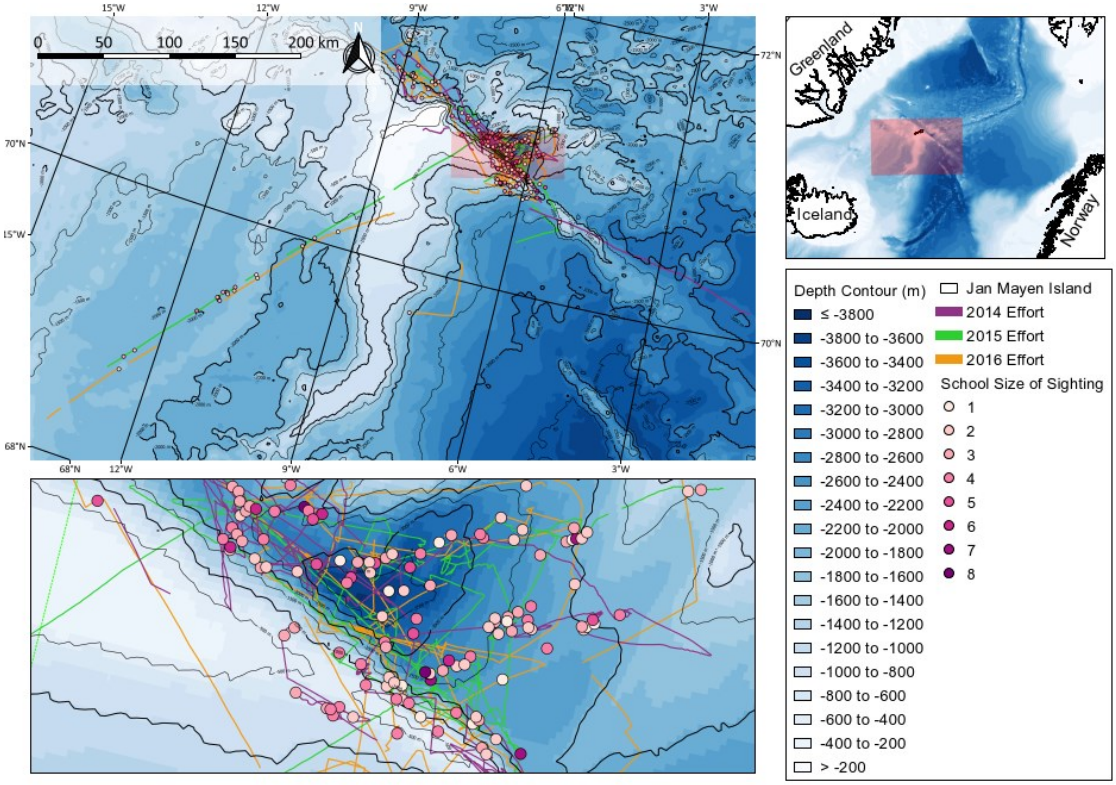

Fig. 1| (Middle panel) The location and number of whale sightings (coloured symbols) and survey effort (coloured lines) by year within the study area off the Jan Mayen Island. (Right) location of the study area relative to Iceland, Greenland and Norway. (Bottom panel) Zoomed map illustrating the dense sighting records made along the submarine canyon to southeast of the Jan Mayen Island.

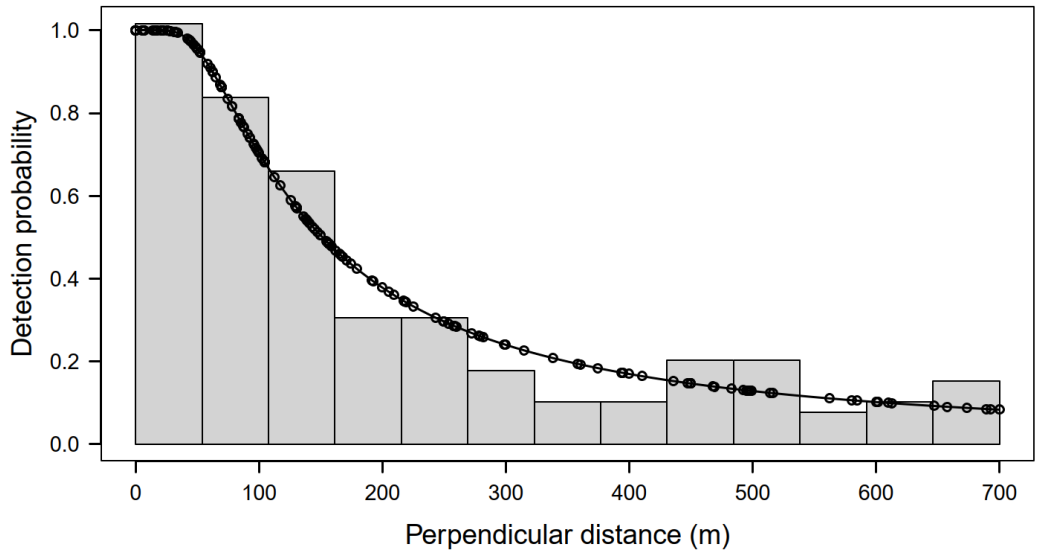

Fig. 2| Detection function fit for the hazard-rate CDS model with truncation distance 700 m. Open circles indicate perpendicular distances of sightings, and the smoothed curve is the fitted detection function.

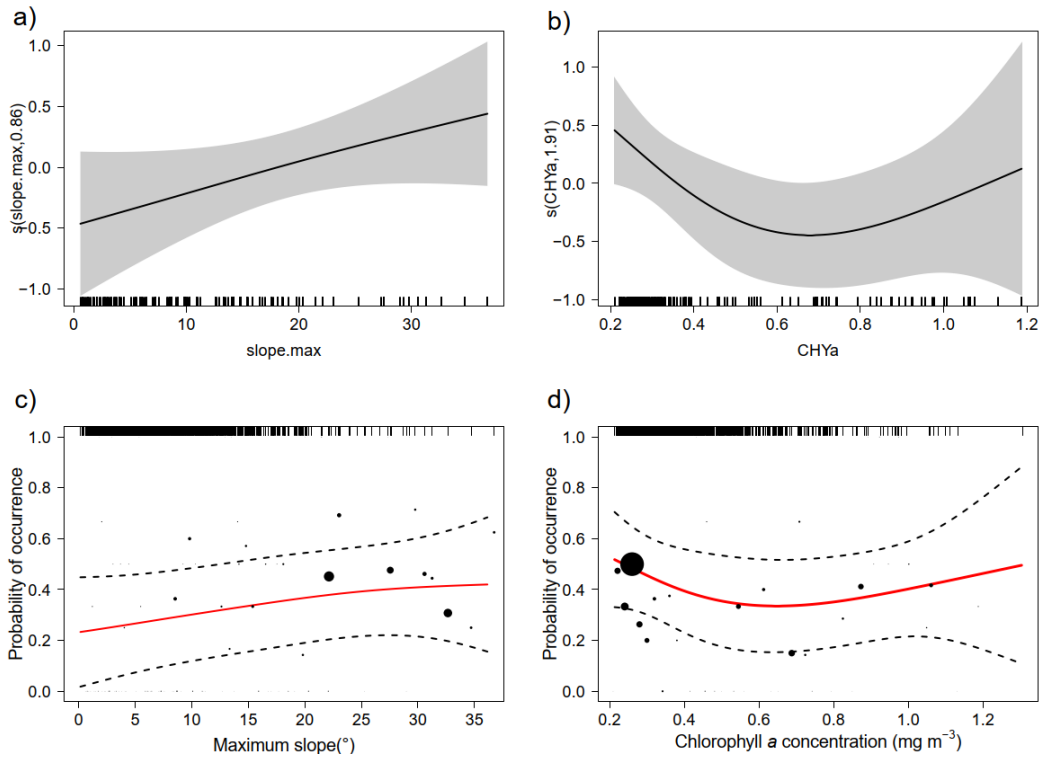

Fig. 3| Component smooth functions of a) maximum slope in degree (°); and b) April chlorophyll concentration in mg m^{-3}. Model-averaged estimates (red curves) of occurrence probability as a function of c) slope; d) April chlorophyll concentration throughout environmental predictor ranges, given the mean values of other covariates. Solid lines represent the smooth estimates, with shaded bands in a) and b) and dash lines in c) and d) representing the intervals of ± 2 standard errors. Dots in c) and d) indicate original data with dot size proportional to the sample size within the defined bins.

809

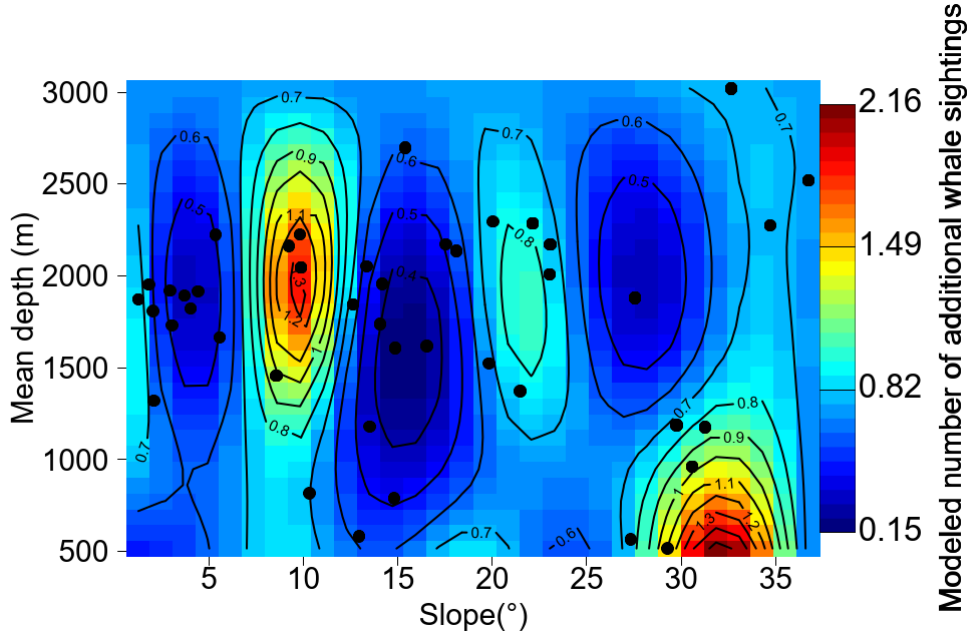

810

811 **Fig. 4| Modeled values of additional whale sightings given first encounter on the response**
812 **scale, as a function of the interaction between mean depth and slope. Black points**
813 **represent whale–present observations.**

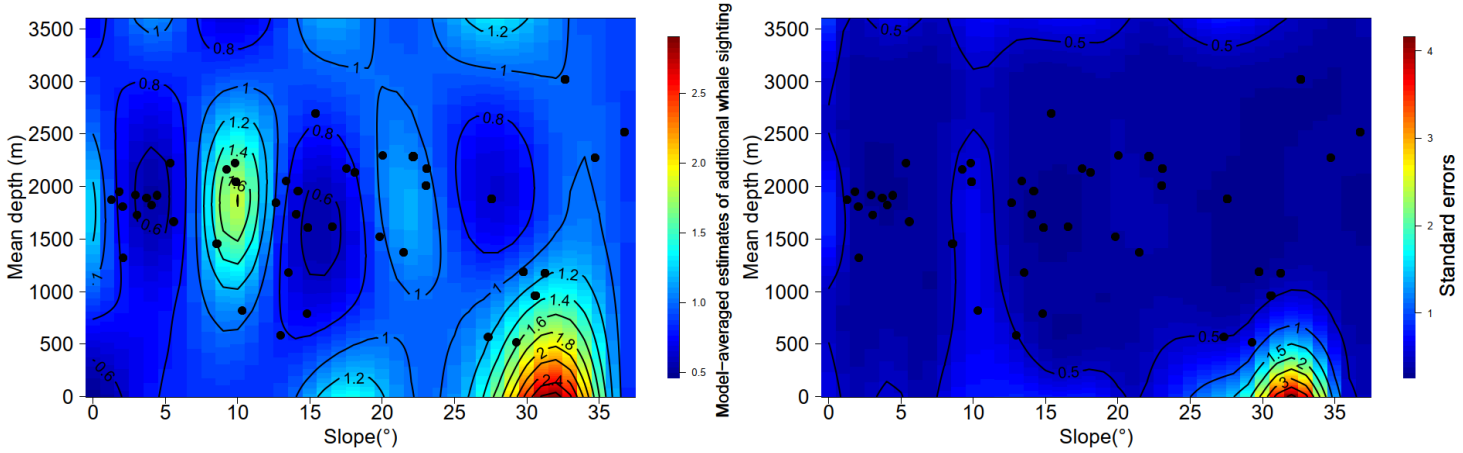

814 **Fig. 5| a) Model-averaged estimates of additional whale sightings given first encounter as**
815 **a function of the depth-slope interaction term and b) associated standard error values.**
816 **Black points represent whale–present observations.**

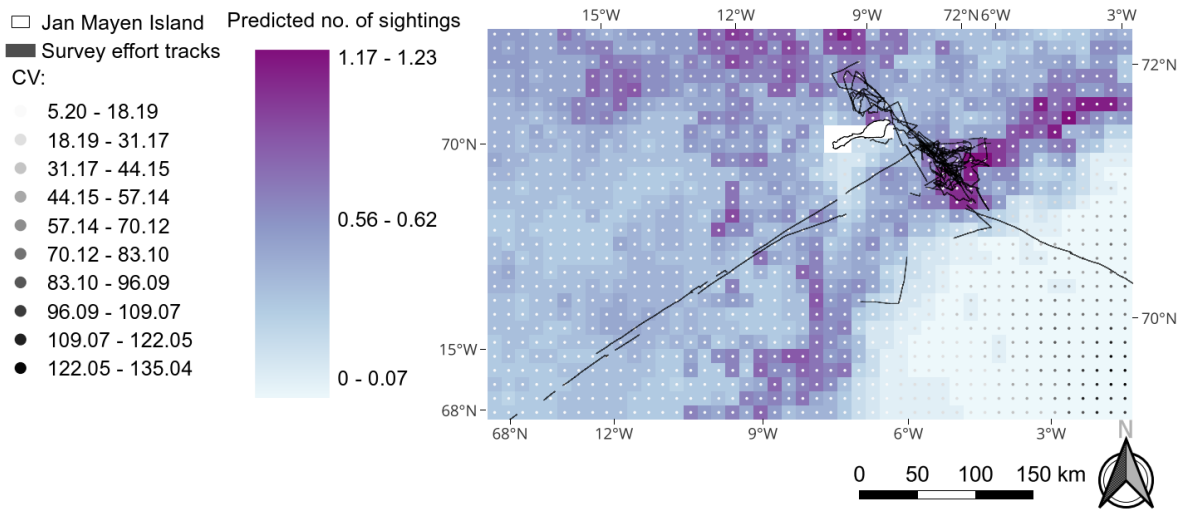

817

818 **Fig. 6| Spatial estimates of number of whale sightings over the wider prediction area,**
819 **based upon the observed pattern of sightings in the smaller surveyed area covered by**
820 **effort tracks. Model estimates are illustrated by the colour of grid cells. The associated**
821 **coefficient of variation (CV) is represented by centroid point with higher CV values**
822 **indicated by darker dot colour.**